Supporting Information

Comparative study of high-k Metal Oxide-PVP/PMMA hybrid Gate Dielectrics for low-temperature, all-solution-processed flexible In_2O_3 thin film transistors

J. Meza Arroyo[a*], M.G. Syamala Rao[a], V.H. Martínez-Landeros[b], O. Cortázar[a], Julia W. P. Hsu[c], R. Ramírez-Bon[a*]

[a] Centro de Investigación y de Estudios Avanzados del IPN, Unidad Querétaro, Apdo, Postal 1-798, 76001 Querétaro, Querétaro, México.

b Facultad de Metalurgia, Universidad Autónoma de Coahuila, Carr. 57, km. 5, C.P.25720, Monclova, Coahuila, México

[c] Department of Materials Science and Engineering, The University of Texas at Dallas, 800 West Campbell Road, Richardson, Texas 75080, United States

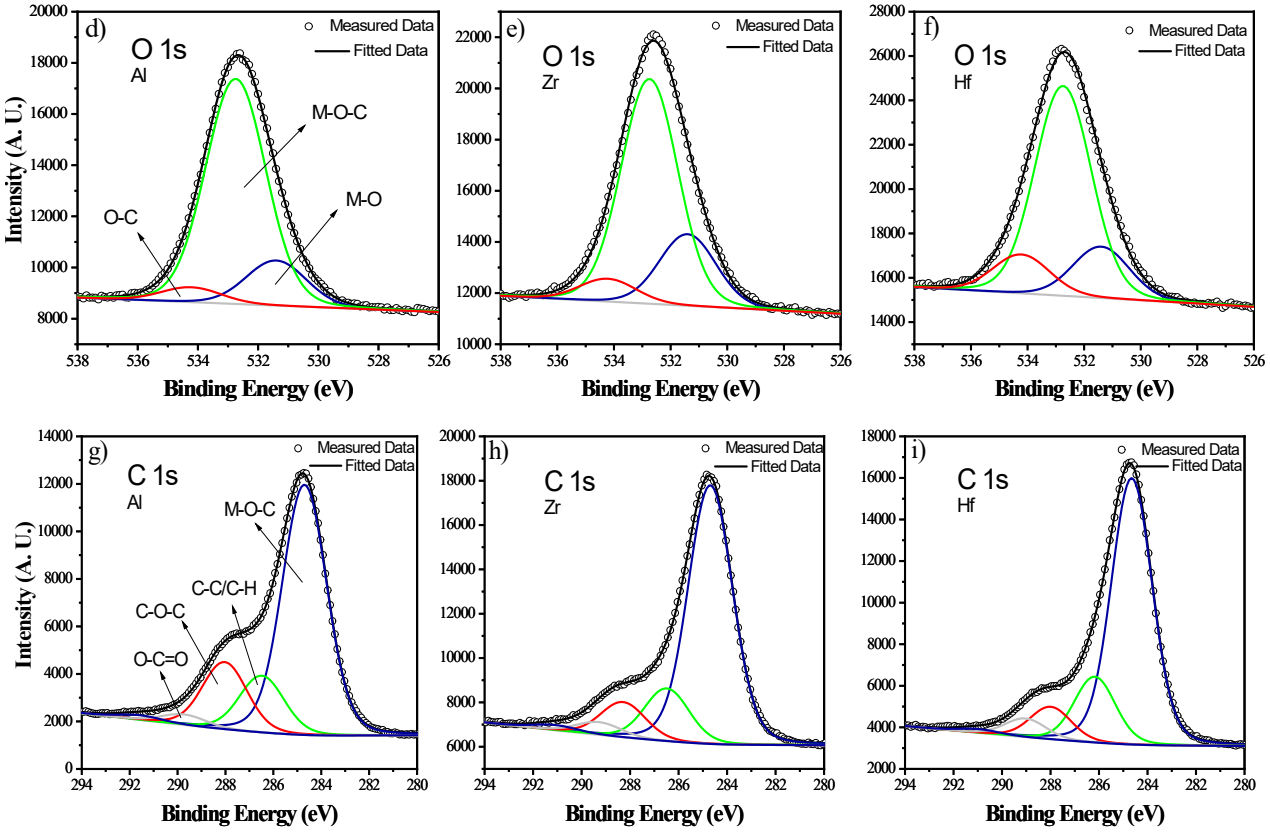

Fig. S1. High resolution XPS spectra of O 1s for d) AlOx, e) ZrOx, and f) HfOx-based hybrid dielectrics, and C 1s for g) AlOx, h) ZrOx, and i) HfOx-based hybrid dielectrics.

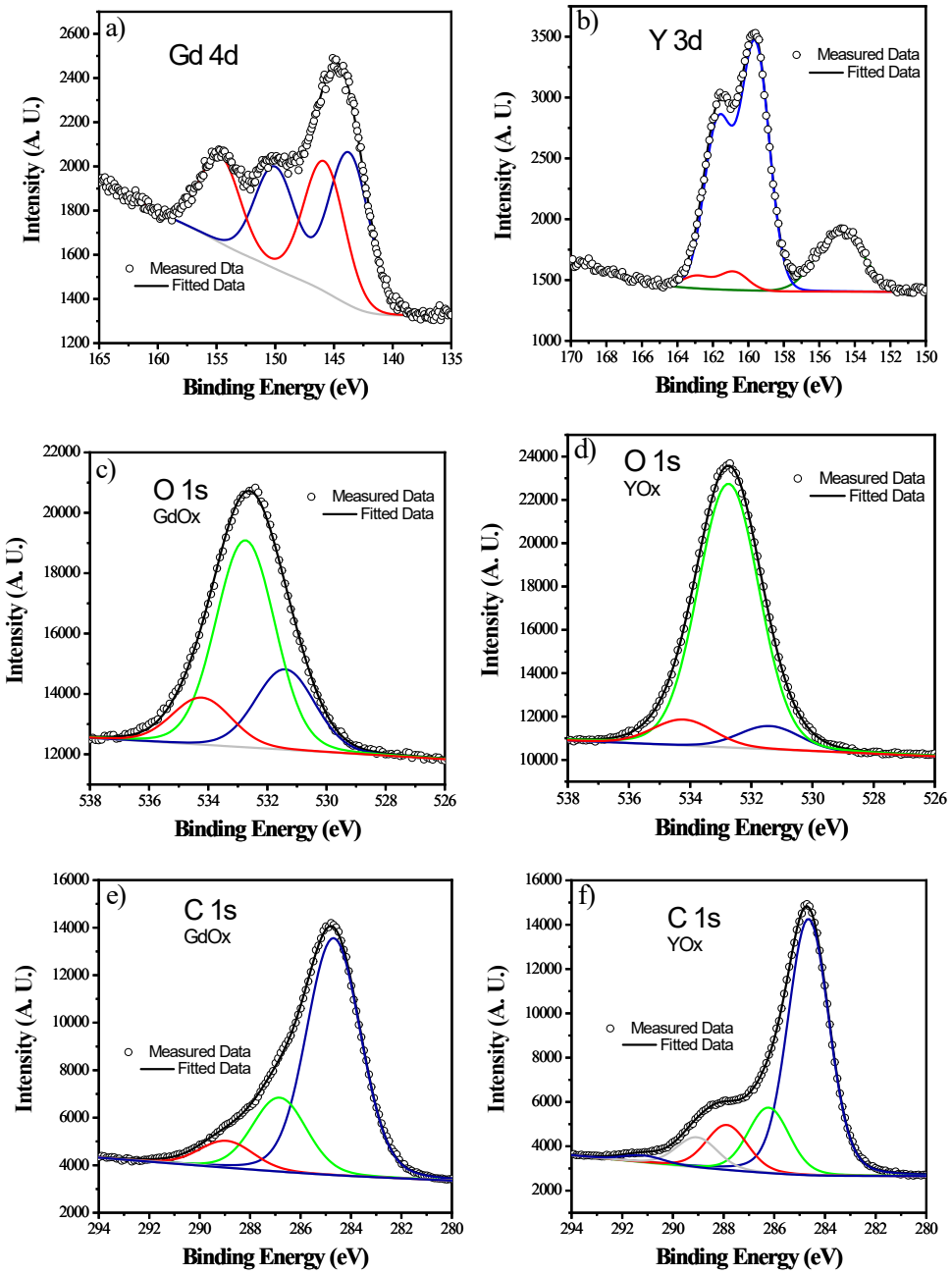

Fig. S2. High resolution XPS spectra of a) Gd 4d, b) Y 3d, O 1s for c) GdOx, and d) YOx-based hybrid dielectrics, and C 1s for e) GdOx, and f) YOx-based hybrid dielectrics.

Table S1 Parameters used for the XPS peak-fitting procedure.

Fitting parameters				***Atomic Porcentage (%)***					
Peak	***Binding Energy (eV)***	***Gaussian***	***Lorentzian***	***PMMA***	***Gd***	***Zr***	***Hf***	***Y***	***Al***
C_1	284.68	1.97	0.35	66.42	50.36	48.10	47.40	39.23	40.75
C_2	286.47	1.97	0.35	9.49	15.67	9.74	11.67	9.99	9.18
C_3	288.02	1.97	0.35	--	5.72	6.57	5.80	6.91	10.93

C_4	289.73	1.97	0.35	--	0.22	2.35	3.30	4.60	1.68
C_5	291.53	1.97	0.35	--	--	0.98	0.65	1.04	0.80

Fitting parameters				***Atomic Porcentage (%)***					
Peak	***Binding Energy (eV)***	***Gaussian***	***Lorentzian***	***PMMA***	***Gd***	***Zr***	***Hf***	***Y***	***Al***
O_1	531.35	2.18	0.25	3.23	4.35	4.44	3.56	1.59	2.61
O_2	532.73	2.18	0.25	8.92	11.71	14.39	15.02	18.17	13.30
O_3	34.25	2.18	0.25	1.60	2.54	1.40	2.69	1.77	0.86

Core	***Peak***	***Branch***	***Binding Energy (eV)***	***Spin-orbit Splitting***	***Gaussian***	***Lorentzian***	***Atomic Porcentage (%)***
Gd 4*d*	Gd_1	5/2	143.69	6.29	3.92	0	0.65
		3/2	149.98		3.92	0	
	Gd_2	5/2	145.79	8.86	3.92	0	0.56
		5/2	154.65		3.92	0	
Zr 3*d*	Zr_1	5/2	183.92	2.4	1.62	0.38	3.14
		3/2	186.32		1.62	0.38	
	Zr_2	5/2	185.44	2.4	1.62	0.02	0.24
		3/2	187.84		1.62	0.02	
Hf 4*f*	Hf_1	7/2	19.38	1.66	1.89	0.13	0.19
		5/2	21.04		1.89	0.13	
	Hf_2	7/2	21.93	1.66	1.89	0.13	3.92
		5/2	23.59		1.89	0.13	
Y 3*d*	Y_1	5/2	159.59	2.09	1.79	0.047	3.08
		3/2	161.68		1.79	0.047	
	Y_2	5/2	160.84	2.09	1.79	0.047	0.22
		3/2	162.93		1.79	0.047	
Al 2*p*	Al_1	3/2	75.87	0.44	2.48	0.085	2.37
		1/2	76.31		2.48	0.085	

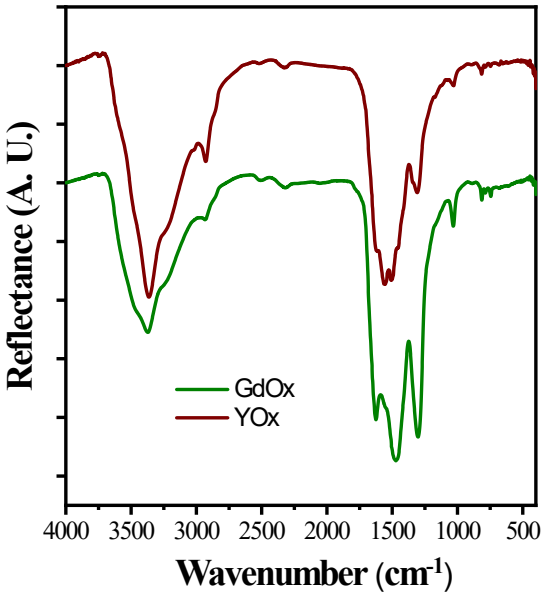

Fig. S3. FTIR spectra of GdOx/PVP-PMMA and YOx/PVP-PMMA hybrid films

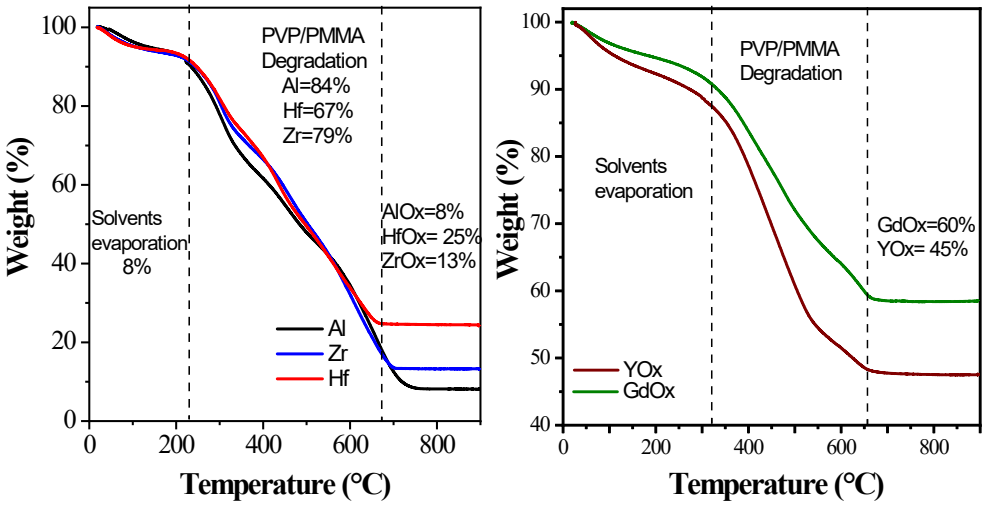

Fig. S4. TGA curves of hybrid dielectrics

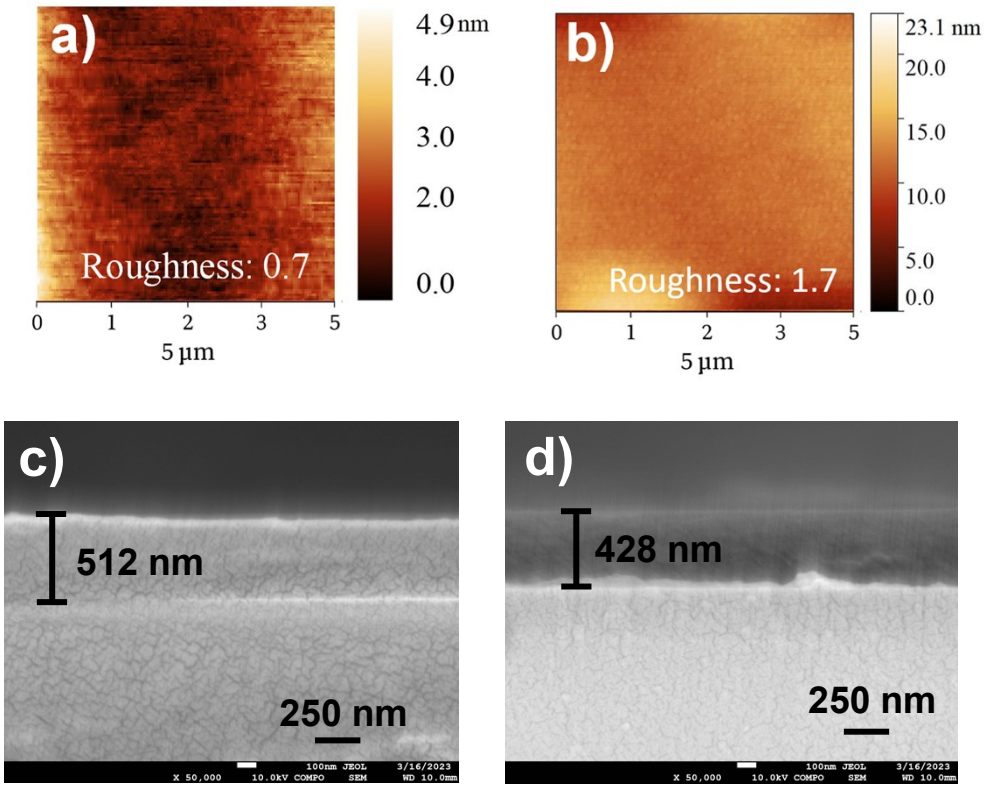

Fig. S5. AFM surface images of a) GdOx-PVP/PMMA, and b) YOx-PVP/PMMA hybrid dielectrics. Cross sectional SEM images of c) GdOx-PVP/PMMA, and d) YOx-PVP/PMMA

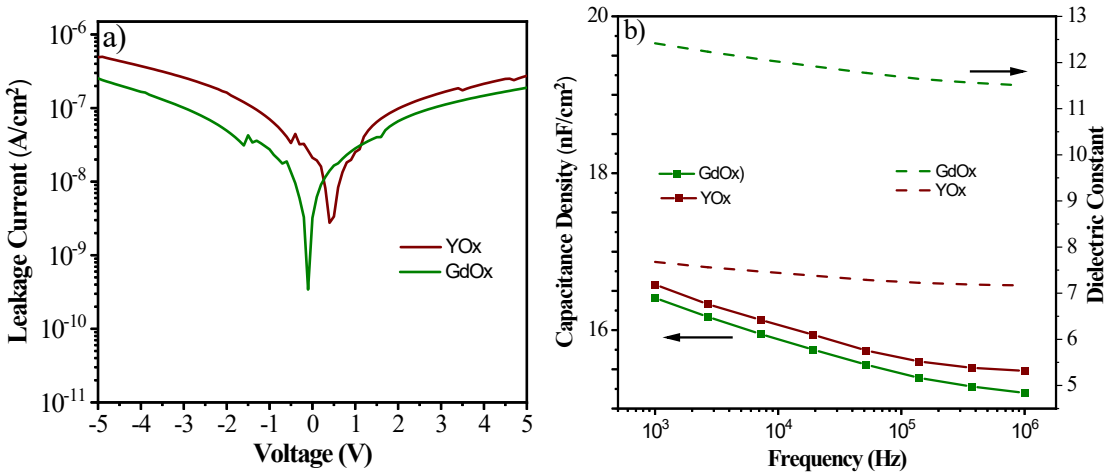

Fig. S6. a) Current density versus voltage and b) capacitance density and dielectric constant versus frequency characteristics of GdOx-PVP/PMMA and YOx-PVP/PMMA hybrid thin films.

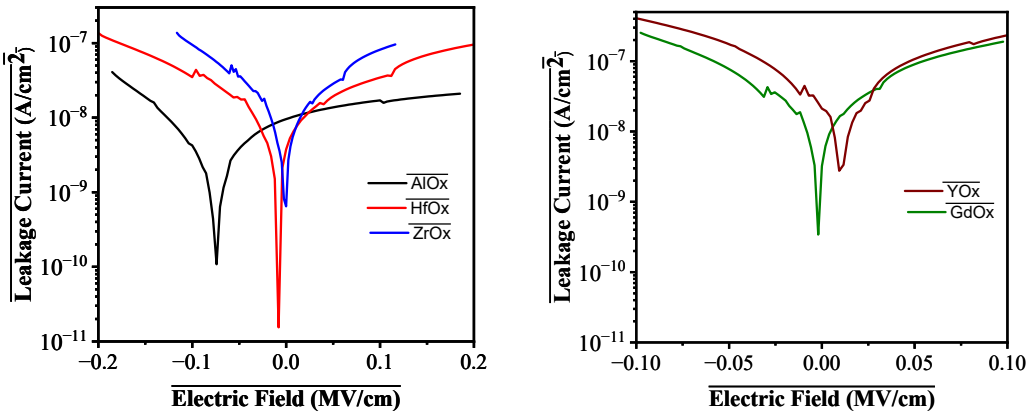

Fig. S7. a) Current density versus electric field of MOx-PVP/PMMA hybrid thin films.

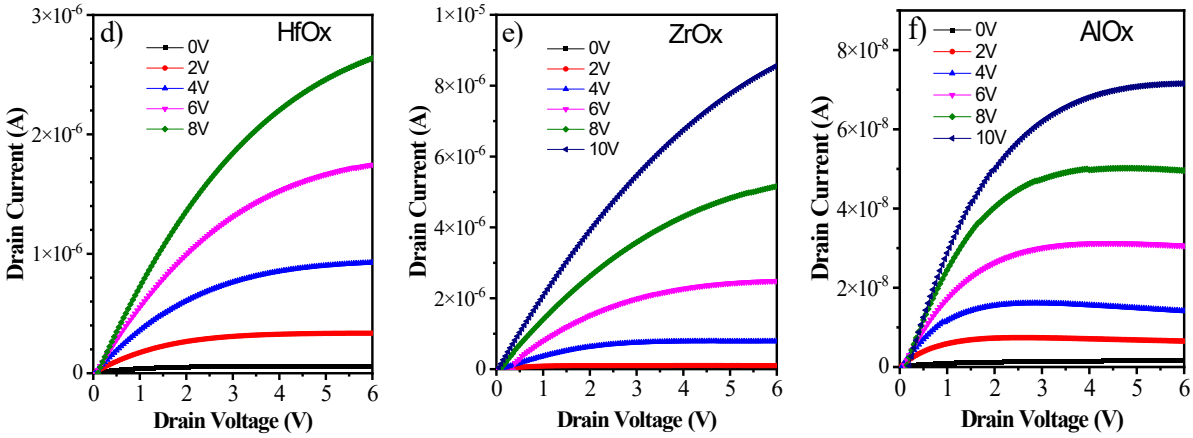

Fig. S8. Output curves of d) HfOx-PVP/PMMA, e) ZrOx-PVP/PMMA, and f) AlOx-PVP/PMMA gate dielectrics.

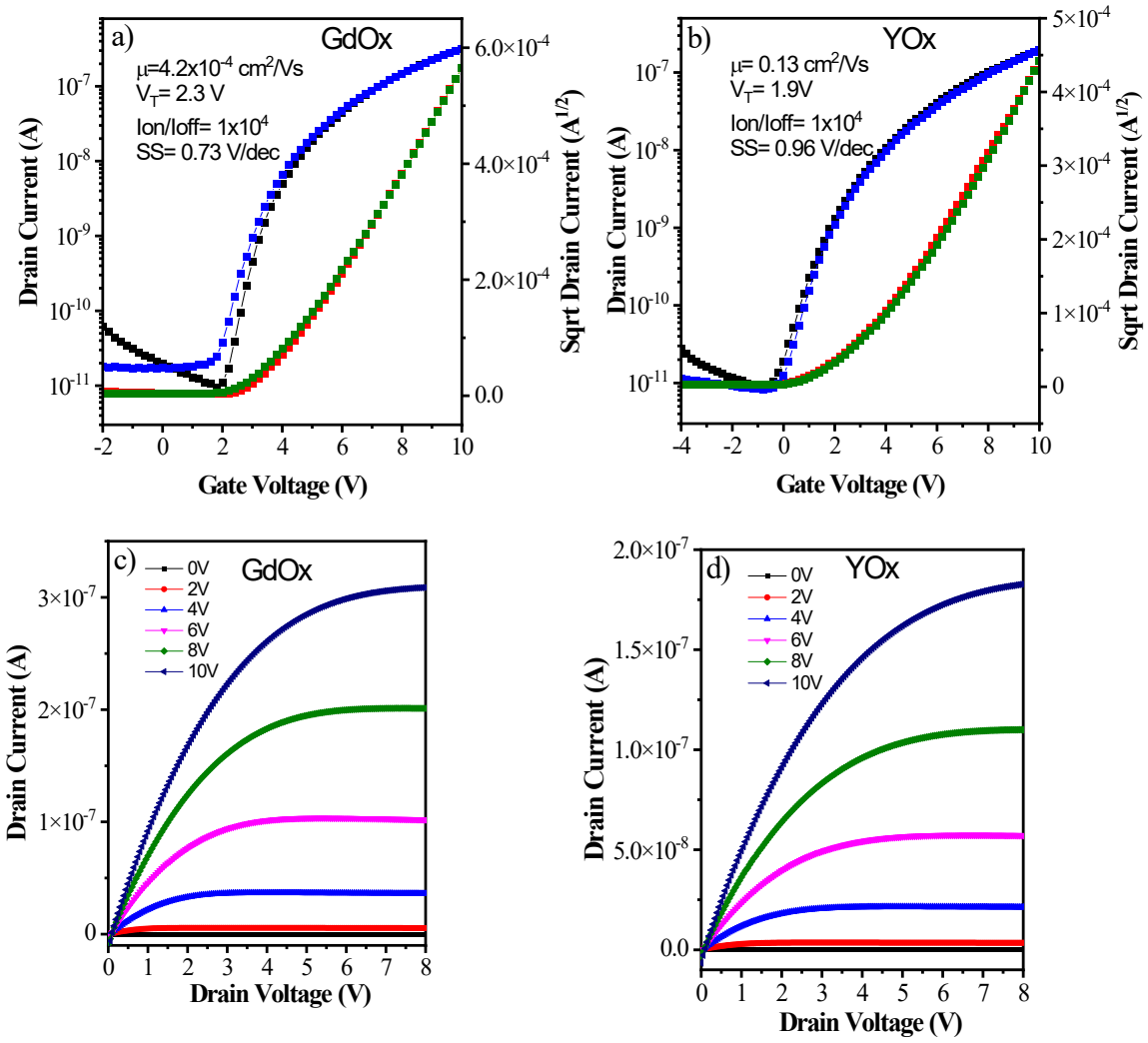

Fig. S9. Transfer curves of the In_2O_3-based TFTs with a) GdOx-PVP/PMMA, and b) YOx-PVP/PMMA gate dielectrics, and corresponding output curves of c) GdOx-PVP/PMMA, and d) YOx-PVP/PMMA gate dielectrics.

Table S2. Electrical performance parameter obtained for the In_2O_3-based TFT over rigid substrates.

Sample	Mobility (cm^2/Vs)	Threshold Voltage (V)	Subthreshold swing (V/dec)	I_{ON}/I_{OFF}
GdOx	4.3e-4	2.3	0.73	10^4
YOx	0.13	1.9	0.97	10^4

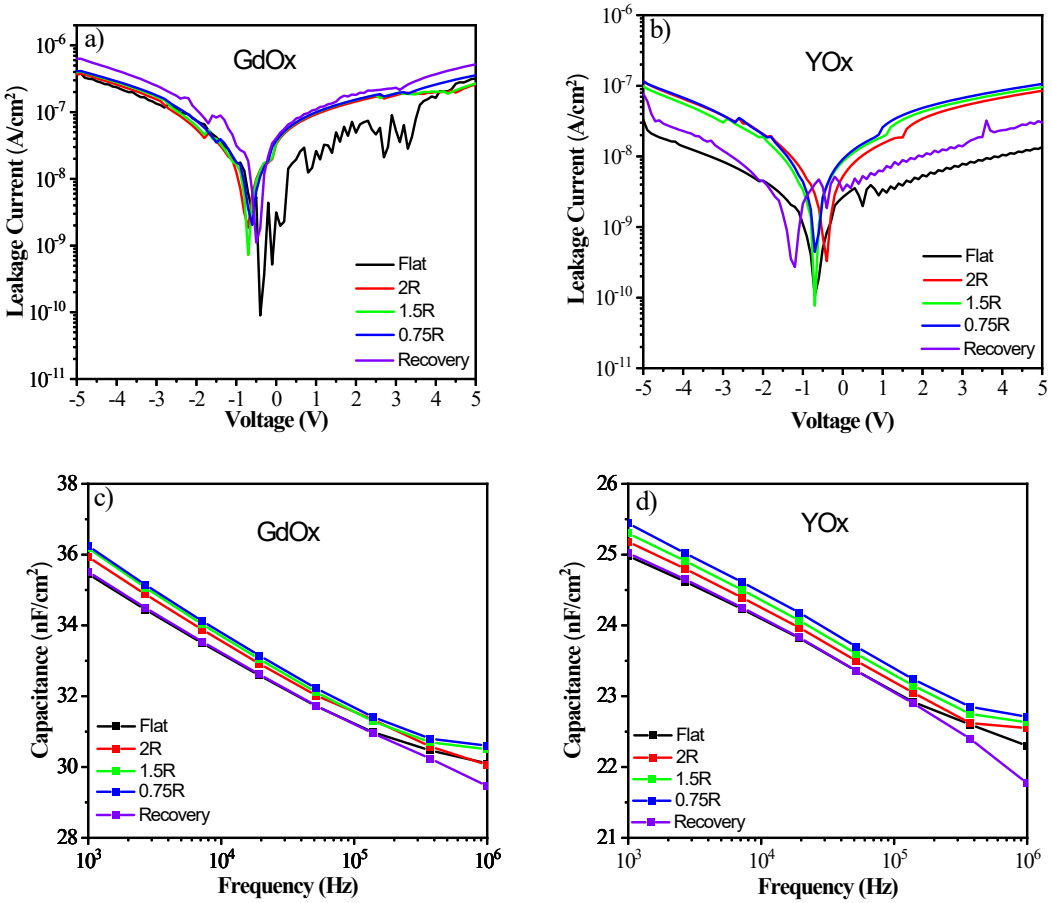

Fig. S10. Current density versus voltage measured at different bending radii on MIM structures fabricated on Al-coated PEN flexible substrate with a) GdOx-PVP/PMMA, and b) YOx-PVP/PMMA. Capacitance density versus frequency measured at different bending radii on the flexible MIM with c) GdOx-PVP/PMMA, and d) YOx-PVP/PMMA hybrid insulators.

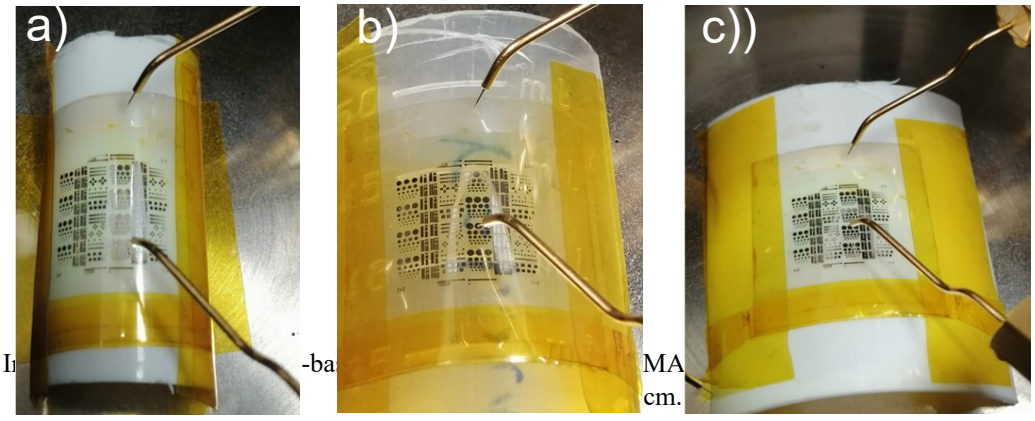

Fig. S11. I -ba MA radii: a) 0.75 cm.

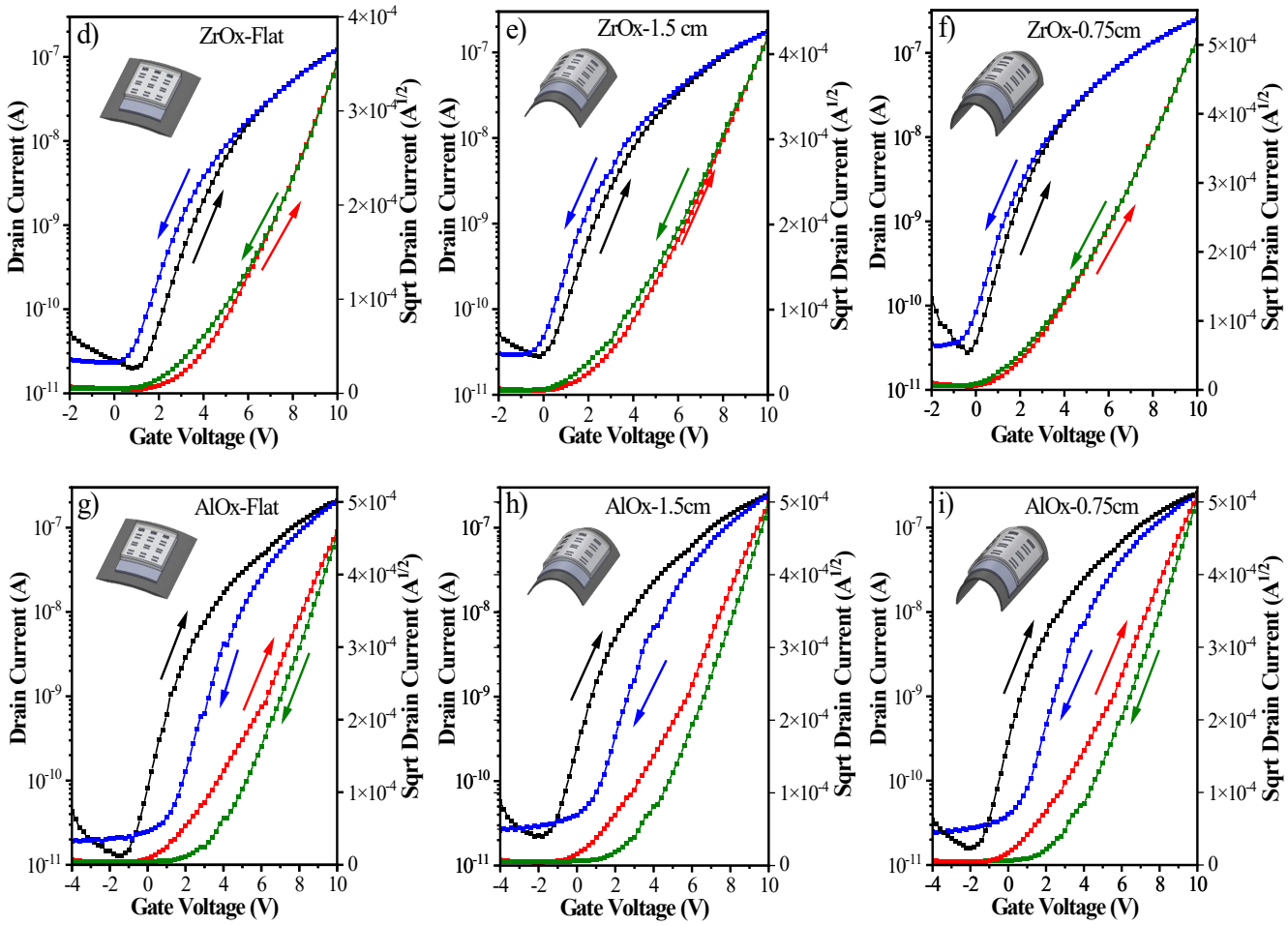

Fig. 12. Transfer curves (left axis) and Sqrt Drain Current versus Gate Voltage (right axis) of the In_2O_3-based TFTs with ZrOx-PVP/PMMA and AlOx-PVP/PMMA gate dielectrics, measured at different bending radii: a) and d) without bending, b), and e) 1.5 cm, and c) and f) 0.75 cm, respectively.

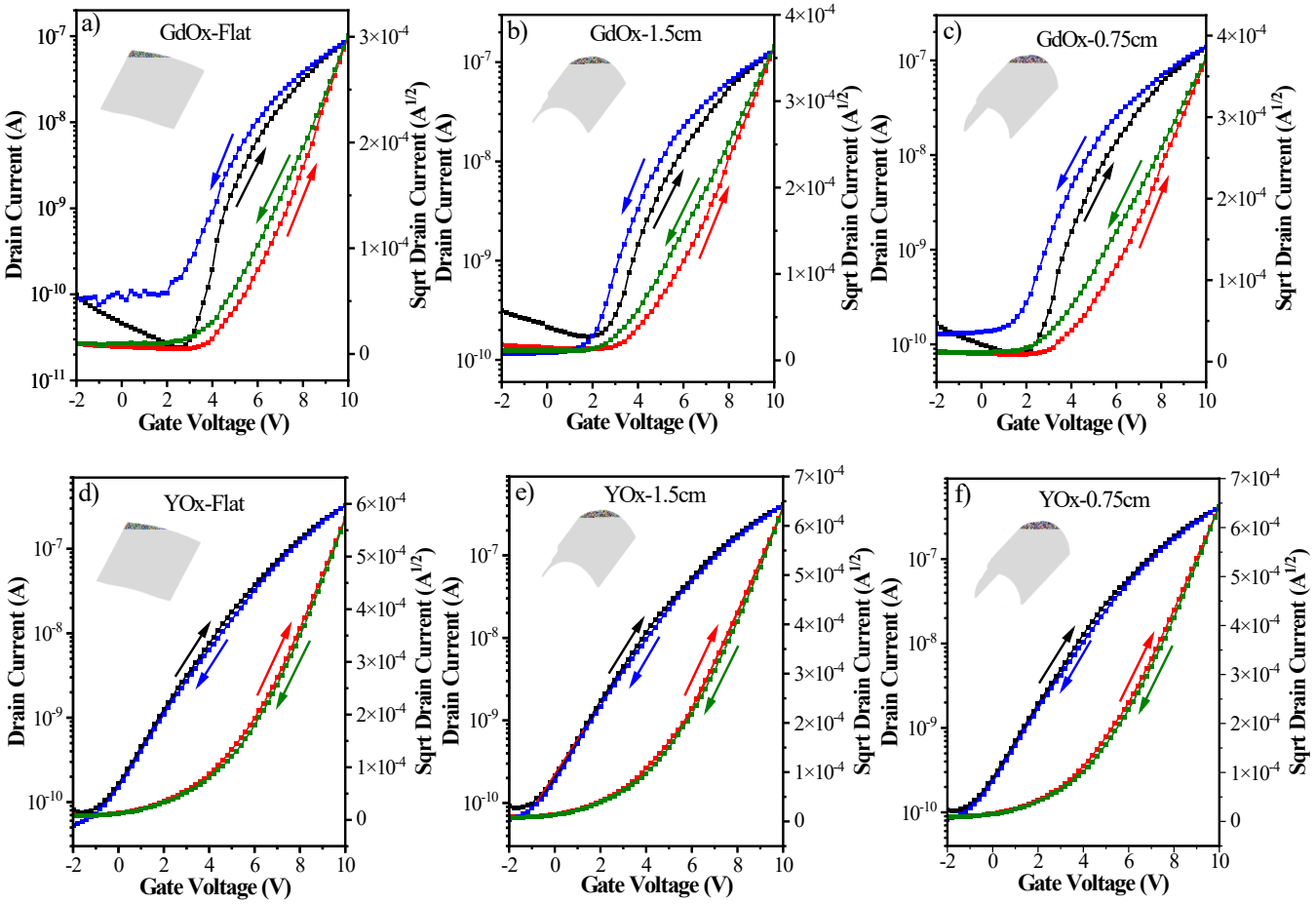

Fig. S13. Transfer curves (left axis) and Sqrt Drain Current versus Gate Voltage (right axis) of the In_2O_3-based TFTs with GdOx-PVP/PMMA, and YOx-PVP/PMMA gate dielectrics, measured at different bending radii: a), and d) without bending, and b), and e) 1.5 cm, and c), and f) 0.75 cm, respectively.

Table S3. Parameters obtained for the In_2O_3-based TFT over flexible substrates under bending conditions.

Sample	Bending Radii (cm)	Mobility (cm^2/Vs)	V_T (V)	SS (V/dec)	I_{ON}/I_{OFF}
GdOx-PVP/PMMA	Flat	1.06E-02	4.6	1.01	4.00E+03
	2R	1.18E-02	4.04	1.35	1.92E+03
	1.5R	1.77E-02	3.98	1.54	7.38E+02
	0.75R	1.86E-02	3.98	1.37	1.60E+03
	Recover	2.95E-03	4.6	1.18	2.98E+03
YOx-PVP/PMMA	Flat	6.48E-02	4.1	2.56	4.13E+03
	2R	6.98E-02	3.9	2.50	5.85E+03
	1.5R	7.08E-02	3.9	2.38	4.53E+03
	0.75R	7.05E-02	3.7	2.50	3.90E+03
	Recover	7.06E-03	4.0	2.13	6.60E+03